

On the incidence of weak magnetic fields in DA white dwarfs[★]

J. D. Landstreet^{1,2}, S. Bagnulo¹, G. G. Valyavin³, L. Fossati⁴, S. Jordan⁵, D. Monin⁶, and G. A. Wade⁷

¹ Armagh Observatory, College Hill, Armagh, BT61 9DG, Northern Ireland, UK
e-mail: sba@arm.ac.uk

² Department of Physics and Astronomy, The University of Western Ontario, London, Ontario, N6A 3K7, Canada
e-mail: jlandstr@uwo.ca; jls@arm.ac.uk

³ Special Astrophysical Observatory, Nizhnij Arkhyz, Zelenchukskiy Region, Karachai-Cherkessian Republic, Russia 369167
e-mail: gvalyavin@sao.ru

⁴ Argelander-Institut für Astronomie der Universität Bonn, Auf dem Hügel 71, 53121 Bonn, Germany
e-mail: lfossati@astro.uni-bonn.de

⁵ Astronomisches Rechen-Institut, Zentrum für Astronomie der Universität Heidelberg, Mönchhofstr. 12-14, D-69120 Heidelberg, Germany
e-mail: jordan@ari.uni-heidelberg.de

⁶ Dominion Astrophysical Observatory, Herzberg Institute of Astrophysics, National Research Council of Canada, 5071 West Saanich Road, Victoria, BC V9E 2E7, Canada
e-mail: dmitry.monin@nrc.gc.ca

⁷ Department of Physics, Royal Military College of Canada, PO Box 17000, Stn Forces, Kingston, Ontario K7K 7B4, Canada
e-mail: gregg.wade@rmc.ca

Received June 18, 2012; accepted July 29, 2012

ABSTRACT

Context. About 10 % of white dwarfs have magnetic fields with strength in the range between about 10^5 and $5 \cdot 10^8$ G. It is not known whether the remaining white dwarfs are not magnetic, or if they have magnetic fields too weak to be detected with the techniques adopted in the large surveys. Information is particularly lacking for the cooler (and generally fainter) white dwarfs.

Aims. We describe the results of the first survey specifically devised to clarify the detection frequency of kG-level magnetic fields in cool DA white dwarfs.

Methods. Using the FORS1 instrument of the ESO VLT, we have obtained Balmer line circular spectropolarimetric measurements of a small sample of cool (DA6 – DA8) white dwarfs. Using FORS and UVES archive data, we have also revised numerous white dwarf field measurements previously published in the literature.

Results. We have discovered an apparently constant longitudinal magnetic field of ~ 9.5 kG in the DA6 white dwarf WD 2105–820. This star is the first weak-field white dwarf that has been observed sufficiently to roughly determine the characteristics of its field. The available data are consistent with a simple dipolar morphology with magnetic axis nearly parallel to the rotation axis, and a polar strength of ≈ 56 kG. Our re-evaluation of the FORS archive data for white dwarfs indicates that longitudinal magnetic fields weaker than 10 kG have previously been correctly identified in at least three white dwarfs. However, for one of these three weak-field stars (WD 2359–434), UVES archive data show a ~ 100 kG mean field modulus. Either at the time of the FORS observations the star's magnetic field axis was nearly perpendicular to the line of sight, or the star's magnetic field has rather complex structure.

Conclusions. We find that the probability of detecting a field of kG strength in a DA white dwarf is of the order of 10 % for each of the cool and hot DA stars. If there is a lower cutoff to field strength in white dwarfs, or a field below which all white dwarfs are magnetic, the current precision of measurements is not yet sufficient to reveal it.

Key words. Stars:white dwarfs – Stars:magnetic field

1. Introduction

In 1970, a magnetic field was discovered in the peculiar white dwarf (WD) Grw +70 8247 = GJ 472 (Kemp et al. 1970). The field strength was eventually estimated to be of the order of 300 MG (Greenstein 1984; Wickramasinghe & Ferrario 1988; Jordan 1992). Since this first detection of a magnetic field in a degenerate star, about 200 magnetic white dwarfs (MWDs) have been discovered (Kawka et al. 2007; Külebi et al. 2009b). It is found that about 10 % of all single WDs have a magnetic field

with a strength in the range between hundreds of kG and hundreds of MG.

It is not at all clear how the magnetic fields in WDs originate, nor what information they carry about the origin and evolution of magnetism during stellar evolution. It is also not very clear yet how these fields influence such phenomena as rotation periods or pulsation of white dwarfs. Clearly, a broad observational base of data is essential for understanding these issues.

The magnetic fields of WDs are sometimes variable with the stellar rotation period, which when measurable is typically of the order of hours or days (e.g. Kawka et al. 2007). It appears that MWDs may often be somewhat more massive than the overall WD average mass of about $0.6 M_{\odot}$ (Liebert 1988), although fields are occasionally found in relatively low-mass WDs. Most of the fields known are in WDs of spectral type DA, a white

[★] Based on observations collected at the European Organisation for Astronomical Research in the Southern Hemisphere, Chile, under observing programme 073.D-0516, and obtained from the ESO/ST-ECF Science Archive Facility.

dwarf classification indicating that the optical spectrum shows only spectral lines of hydrogen, and which generally identifies WDs with H-rich atmospheres. This is at least partly a selection effect due to the fact that the strong and sharp Balmer lines are particularly sensitive probes of stellar magnetism, which in many cases can be easily detected in low-dispersion spectra from surveys such as the Sloan Digital Sky Survey (Külebi et al. 2009a,b).

The concentration of WD magnetic field strengths as a function of $\log(|B|)$ (Külebi et al. 2009b) in the best-studied range of 1–100 MG has raised the question of whether there is a cut-off field strength below which white dwarf fields do not occur (as is the case for Ap stars, Aurière et al. 2007), or whether the probability of detecting a field might rise sharply below a field strength of some tens of kG. Resolving this question confronts the difficulty of detecting weak fields in such faint, broad-lined objects, and our current knowledge of the low-field tail of the white dwarf field strength distribution is limited mainly by instrumental constraints. It is very difficult to obtain field measurements with standard errors of less than about 10 kG without using the largest available telescopes (see e.g. Valyavin et al. 2006; Kawka et al. 2007). However, the study of available statistics by Liebert et al. (2003) and the survey by Aznar Cuadrado et al. (2004) both suggest that the detection rate for field weaker than a few tens of kG may be significantly higher than the frequency of $\sim 10\%$, which characterises the overall detection rate of stronger fields.

A further question of great interest is whether the magnetic fields of WDs evolve with time, and if so, how they evolve. The searches for kG fields reported so far (Aznar Cuadrado et al. 2004; Valyavin et al. 2006; Kawka et al. 2007; Jordan et al. 2007) have focussed almost entirely on the generally brighter hotter (and therefore younger) white dwarfs. It is thus worthwhile to focus a survey on cooler and older white dwarfs, and the higher detection probability predicted by earlier work suggests that even a fairly small sample of such stars may yield interesting results.

Thus, to increase the available information about the incidence of weak fields, and to extend this information to include some older, cooler white dwarfs, we have carried out a modest survey for fields in DA WDs with effective temperatures T_{eff} below about 14 000 K, aiming at obtaining field measurements with ~ 1 kG error bars.

Recent work by Bagnulo et al. (2012), Jordan et al. (2012), and Landstreet et al. (2012) have shown that the results of some FORS1 surveys of magnetic fields in various classes of stars were affected by spurious detections, highlighting the need for a re-analysis of published data for MWDs. Therefore, we have complemented the results of our own survey with the revision of all FORS1 field measurements of WDs.

2. New observations

White dwarfs with very strong fields can be identified via broadband circular polarimetry, as magnetic fields may produce circular polarization of the continuum radiation at the level of 1 to a few % for fields of 10 MG or more. However, most MWDs have been detected by observing the Zeeman effect in the Stokes I and/or V profiles of spectral lines.

For a 100 kG magnetic field, the $\pi - \sigma$ separation produced by the Zeeman effect in optical spectral lines is $\sim 1 \text{ \AA}$. For DA WDs, this is of the same order as the pressure broadening of the Balmer line cores (Koester et al. 1998). This sets a lower limit to the strength of the field that can be detected through intensity

measurements, since for a field strength $\lesssim 30$ kG, Zeeman splitting no longer dominates over pressure broadening, and weak splitting is difficult to distinguish from rotational line broadening. Practically, most past surveys could firmly detect only fields with $\langle |B| \rangle \gtrsim 50 - 100$ kG, as at lower field strength the Zeeman splitting in Stokes I would be beneath the resolving-power limit of the instrument, and/or swamped by noise.

In conclusion, for field with strength $\lesssim 50$ kG, the most appropriate method for field detection is based on low-resolution, high signal-to-noise ratio (S/N) measurements of the circular polarization of spectral lines, which can be obtained with large telescopes (Landstreet 1992; Schmidt 2001). Circular spectropolarimetry of Balmer lines is the tool best suited for our field survey of DA stars.

Our circular spectropolarimetric observations (programme ID 073.D-0516) were carried out in service mode during 2004 using FORS1 on the ESO VLT telescope Antu. Our survey draws randomly on a list of nearby cool ($T_{\text{eff}} \lesssim 14\,000$ K) WDs¹. Targets were observed using grism 600B with a 1.0-arcsec slit. Our FORS spectra have a resolving power of about 830, and cover the wavelength window from 3470 to 5880 Å, thus including all the hydrogen Balmer lines from H β down to the series limit at about H9.

For each stellar observations, we typically obtained four integrations with the quarter-wave plate rotated by 90° between successive exposures (an observing procedure that makes it possible to eliminate a number of sources of measurement error to first order – see, e.g., Bagnulo et al. 2009). Data reduction and field measurements were performed as explained by Bagnulo et al. (2012). In particular, the mean line-of-sight magnetic field $\langle B_z \rangle$ was obtained by using the relationship

$$V(\lambda) = -g_{\text{eff}} C_Z \lambda^2 \frac{dI(\lambda)}{d\lambda} \langle B_z \rangle \quad (1)$$

(Landstreet 1982), where $C_Z = e/4\pi mc^2$, as a correlation equation between the slope $dI/d\lambda$ of the local spectral intensity $I(\lambda)$, and the local circular polarisation $V(\lambda)$, pixel by pixel, as explained in detail by Bagnulo et al. (2012). However, in computing the slope of the correlation between the value of V/I with $dI/d\lambda$, sigma clipping has now been introduced to remove outliers (mostly from cosmic rays) that add noise but no real signal. Since all of the stars observed are DA stars, real magnetic signal is only found in the H lines, and therefore field strengths were determined using only these lines. The wavelength window to use for each line of each star was set after visual inspection of the I spectrum, to include all of each line wing out to the point where the line slope decreases to typical values produced by noise in the continuum.

For each observation we have also produced a null spectrum N_V , a quantity computed by combining the circular polarisation spectra from the four sub-exposures of the observation in such a way as to cancel out the the real circular polarisation signal. The value of the null spectrum is that it can reveal artefacts or systematic errors in the data (due for example to cosmic rays). In a successful observation the N_V spectrum should be featureless at the level of the photon noise, and the magnetic field deduced from N_V should be consistent with zero within its uncertainty. The computation and meaning of N_V are discussed at length by Bagnulo et al. (2009, 2012).

The target list, observing log, and field measurements are given in Table 1, which provides: two names (cols. 1 and 2);

¹ Our programme was granted the status of “filler”, and only a fraction of the observations originally planned were actually carried out.

Table 1. New longitudinal magnetic field measurements obtained with FORS1.

Star names		V	Spectral type	T_{eff}	$\log g$	MJD	t_{int}	$\langle B_z \rangle$	$ \langle B_z \rangle / \sigma_{\langle B_z \rangle} $
		(mag)		(K)			(s)	(G)	
WD 1425–811	GJ 2108	13.0	DA6:V	12098	8.21	53137.044	960	488 ± 1360	0.36
WD 1733–544	GJ 4012	15.8	DA8:CV	6165	7.23	53199.178	1664	4104 ± 4390	0.94
WD 1826–045	G 21-16	14.5	DA6	9057	7.99	53193.179	1920	-2705 ± 1530	1.76
WD 1952–206	LTT 7873	15.0	DA6	13184	7.82	53251.088	2840	530 ± 1180	0.45
WD 2105–820	LTT 8381	13.5	DA6	10794	8.19	53192.269	1760	9274 ± 1375	6.75
						53193.278	1760	11423 ± 995	11.47
						53197.294	880	8173 ± 1630	5.02
						53199.317	880	9130 ± 1490	6.12
						53227.209	1760	9770 ± 845	11.59
WD 2115–560	GJ 4191	14.3	DA6	9625	8.01	53199.342	1664	-1367 ± 1065	1.28
						53227.238	1664	132 ± 955	0.14
WD 2151–015	GJ 4236	14.5	DA6	?	?	53240.174	1840	3941 ± 1910	2.08
						53251.124	1840	-2027 ± 950	2.13
						53252.120	1840	-688 ± 1660	0.41
WD 2333–049	G 157-82	15.9	DA6	10608	8.04	53274.201	1704	5102 ± 5550	0.92

visual magnitude V (col. 3); the spectral class (col. 4); the effective temperature T_{eff} in K and the logarithm of the gravity g in cm s^{-2} , both taken from Lajoie & Bergeron (2007) or Koester et al. (2009); the modified Julian Date (MJD) of the midpoint of each observation (col. 7); the total integration time t_{int} in sec (col. 8); the measured value of the mean longitudinal field strength $\langle B_z \rangle$ and its standard error $\sigma_{\langle B_z \rangle}$ (col. 9); and the significance of the detection, $|\langle B_z \rangle / \sigma_{\langle B_z \rangle}|$. The survey comprises 15 individual measurements of eight different stars, and required about 8 h of telescope time in service mode (out of 42 h originally planned).

The observed WDs are quite faint (their magnitude ranges from $V \sim 13$ to ~ 16), and in some of them, the low values of T_{eff} lead to rather weak Balmer lines. Nevertheless, it may be seen that the precision sought for these measurements has been, to a considerable extent, achieved: all but two of the 15 measurements have standard errors in the range of 800 to 2000 G.

3. Results

3.1. Detection of a kG field in WD 2105–820

Only one of the eight cool DA WDs of Table 1 shows clear evidence of a magnetic field of kG strength, namely WD 2105–820 = GJ 820.1 = LTT 8381, which is a DA6 star with $T_{\text{eff}} = 10800$ K. This star had previously been flagged by Koester et al. (1998) as potentially magnetic, on the basis of showing excess broadening (and possibly Zeeman splitting) in the core of $H\alpha$, although they point out that the observed broadening could instead be due to rapid rotation with $v \sin i = 65 \text{ km s}^{-1}$. For this star, we have five $\langle B_z \rangle$ measurements with a typical (median) standard error of about 1400 G. Our five measurements reveal a longitudinal field $\langle B_z \rangle \approx +9500$ G, with a ~ 1200 G dispersion, similar to the median measurement uncertainty. The significance of the individual detections, $|\langle B_z \rangle / \sigma_{\langle B_z \rangle}|$, ranges from about 5 to more than 10. Even with the problem of occasional outliers among field measurements obtained with FORS1 (see Bagnulo et al. 2012), these detections are sufficiently significant and numerous to allow us to conclude that the field is certainly present.

The I , V/I and N_V spectra of one observation of WD 2105–820 are shown in Fig. 1. One can clearly see the weak S-shaped excursions around zero in V/I at the positions of sev-

eral of the Balmer line cores that reveal the presence of the field of this star. Because our observations have quite low spectral resolution, we cannot detect line splitting in the I spectrum, or structure in the variation of V/I with wavelength, from which to obtain further information about field morphology.

3.2. Other results (non-detections)

Two of the three observations of WD 2151–015 are different from zero at a little more than the 2σ level, hence they do not represent a significant detection. However, the presence in this star of a 2 – 4 kG field cannot be ruled out. All the field measurements for all the remaining stars lie within 2σ of zero field.

4. A revised list of detections of weak magnetic fields in DA white dwarfs

To set the results of our survey into a broader context, we have compiled a list that includes all DA WDs in which, according to this and previous work, a measurement of a non-zero longitudinal magnetic field was obtained with an error bar $\sigma_{\langle B_z \rangle} \lesssim 2 \text{ kG}$.

4.1. FORS1 archive measurements of longitudinal field

The largest database of spectropolarimetric data that have reached a sufficiently high S/N to detect weak fields is that included in the FORS1 data archive. Most WD spectropolarimetric observations were obtained in the context of dedicated surveys (Aznar Cuadrado et al. 2004; Jordan et al. 2007, and this work). In addition to them, the FORS1 data archive includes also four additional spectropolarimetric observations of DA WDs that were obtained mainly for calibration purposes.

To produce a homogeneous dataset incorporating our current understanding of how best to treat FORS1 spectropolarimetry, and to examine the data to see if new reductions reveal any significant fields missed in the earlier reductions, all FORS1 measurements have been re-reduced following the same procedure adopted for the results discussed in Sect. 2 (Bagnulo et al. 2012). As discussed at length in that article, these re-reductions are expected to provide significantly improved field strengths and (especially) uncertainties compared to the initial published reductions. Our 70 “new” measurements from “old” FORS1

Table 2. White dwarfs in which weak fields may be present

Star names	Spectral type	T_{eff} (K)	$\log g$	Field detected? (prev. work)	REF.	Field detected? (this work)	strength range (kG)
WD 0413–077 40 Eri B	DA3	17100	7.95	P	FVB03	NA	NA
WD 0446–789 BPM 3523	DA3	23627	7.69	Y	AJN04	Y	–2.5 to –5.7
WD 1105–048 LTT 4099	DA3	15142	7.85	Y	AJN04, VBF06	P	–7.9 to 3.3
WD 1620–391 CD–38 10980	DA2	24231	8.07	P	JAN07	N	–
WD 2007–303 LTT 7987	DA4	14454	7.86	P	JAN07	N	–
WD 2039–202 LTT 8189	DA2.5	19188	7.93	P	JAN07	N	–
WD 2105–820 LTT 8381	DA6	10794	8.19	Y	t.w.	Y	8.1 to 11.4
WD 2359–434 LTT 9857	DA5	8544	8.44	Y	AJN04	Y	3.1 to 4.1

References. Effective temperatures from Lajoie & Bergeron (2007) or Koester et al. (2009). References for the magnetic field detections are as follow: FVB03: Fabrika et al. (2003); AJN04: Aznar Cuadrado et al. (2004); VBF06: Valyavin et al. (2006); JAN07: Jordan et al. (2007); t.w.: this work.

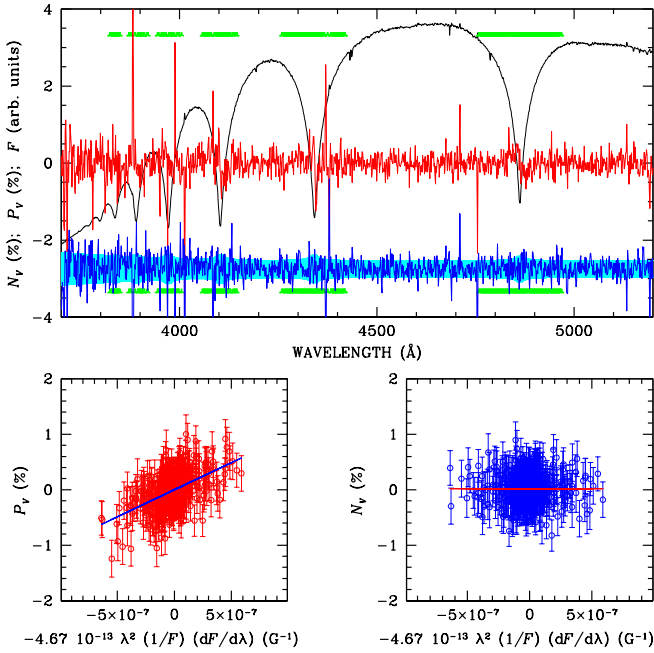


Fig. 1. The observations of WD 2105–820 obtained with FORS1 on 2004-08-10UT 05:01 = MJD 53227.209. The top panel shows the observed flux F (black solid line, in arbitrary units, and not corrected for the instrument response), the $P_V = V/I$ profile (red solid line centred about 0), and the null profile N_V (blue solid line, offset by –2.75% for display purpose). The null profile is expected to be centred about zero and scattered according to a Gaussian with σ given by the P_V error bars, which are represented with light blue bars centred about –2.75%. The regions used for field measurement are marked with green bars above and below this spectrum. The slope of the interpolating lines in the bottom panels provides the mean longitudinal field from P_V (left bottom panel) and from the null profile (right bottom panel) both calculated using only the H Balmer lines. The corresponding $\langle B_z \rangle$ and $\langle N_z \rangle$ values are 9770 ± 843 G and -11 ± 868 G, respectively.

archive data are reported in Table 3 (published online), which is organised in a similar way as Table 1, with the omission of the V magnitude and the insertion of a new column which refers to the ESO programme ID of the observing run cor-

responding the the observation. Values of T_{eff} and $\log g$ are taken from Lajoie & Bergeron (2007); Koester et al. (2009); Giammichele et al. (2012). Note that all our new field determinations from data obtained by Aznar Cuadrado et al. (2004) have the opposite sign compared to their original publication, to conform to the usual sign convention for the mean longitudinal component of a stellar magnetic field (i.e., positive when pointing to the observer).

The result of our re-evaluation of magnetic field measurements in WDs from previously published FORS1 data is to confirm detections in three stars (WD 0446–789, WD 1105–048, and WD 2359–434). Note that these detections are based on rather limited datasets. Each of these stars was observed only twice; in WD 0446–789 and WD 2359–434, a field was detected in both epochs, while in WD 1105–048 the magnetic field was detected only in one of the two observing epochs. All field detections are only at the significance level of 3 to 6σ .

On the basis of $\langle B_z \rangle$ measurements significant at the 2σ to 3σ level, possible fields detections were reported for the stars WD 1620–391, WD 2007–303, and WD 2039–202. In the new reductions, only one of these measurements remains significant at slightly more than the 2σ level. We consider that there is at present no firm evidence that any of these stars possess detected kG fields.

4.2. Other spectropolarimetric observations of weak-field WDs

A literature search for additional WDs with a $\lesssim 20$ kG detected longitudinal magnetic field returned only two stars: WD 0413–077 = 40 Eri B (Fabrika et al. 2003), and one confirming observation for the field of WD 1105–048 (Valyavin et al. 2006).

The detection of WD 0413–077 by Fabrika et al. (2003) is based on an accumulation of measurements, most of which individually are only barely significant. Furthermore, those observations were carried out with rather old spectropolarimeters designed in the late 1970s and early 80s. For these reasons, the detection of the field in WD 0413–011 still requires confirming observations.

The confirming field detection in WD 1105–048 (Valyavin et al. 2006) was obtained within the context of a survey of five WDs (and 2 sdBs), which otherwise reported null results.

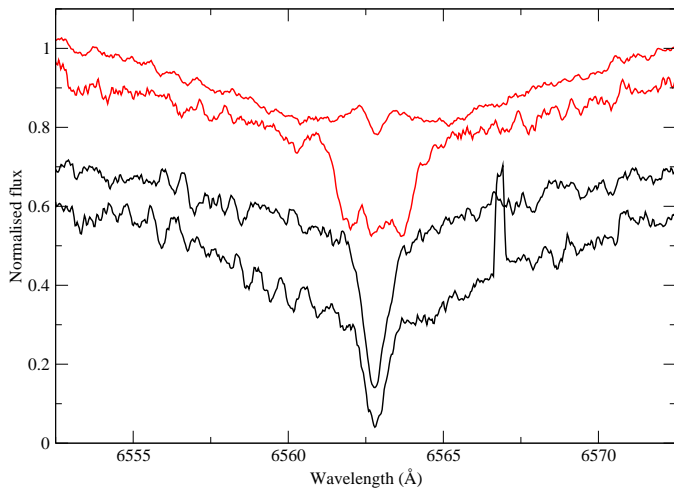


Fig. 2. $H\alpha$ cores of four cool WDs. Top to bottom: WD 2359–434 (magnetic, red line), WD 2105–820 (magnetic, red line), WD 1952–206, WD 1826–045 (both non-magnetic, according to our new FORS data). Spectra are normalised to 1.0 at the edges of the window, then shifted vertically for display purposes.

4.3. A list of white dwarfs with weak magnetic fields

The entries of Table 3, complemented with the WD targets of the survey by Valyavin et al. (2006) and the observation of WD 0413–077 by Fabrika et al. (2003), constitute a database that includes high-precision field measurements for 36 DA WDs. From Table 3 we have excluded four WDs for which $\langle B_z \rangle$ measurements were obtained with error bars substantially larger than 2 kG. The mean error bar is 0.8 kG, which corresponds to a typical (firm) field detection threshold of about 5 kG. From this database we have extracted a final list of suspected or confirmed weak-field DA WDs that satisfy the condition $|\langle B_z \rangle| < 20$ kG. This list of stars (sorted by RA) is given in Table 2, which is organised as follows. Cols. 1 to 4 give star ID, spectral type, effective temperature and gravity. Col. 5 contains a comment as to whether the field measurement that appeared in the original papers would correspond to firm detection (Y), or to a possible detection (P). The publications that include the original field measurements are listed in col. 6. Col. 7 shows a note reporting whether according to our re-reduction of FORS1 data of Table 3, a field was firmly (Y), possibly (P) or not (N) detected. The acronym NA (not applicable) used for 40 Eri B means that the original data were not obtained with FORS and were not re-analysed. Col. 8 provides a new estimate of the range of field variation as determined from the measurements available to date, including the revisions reported in Table 3.

Table 2 shows that the newly-detected weak-field white dwarf, WD 2105–082, has been observed sufficiently often, and with sufficiently high precision to fully confirm the existence of the detected field, and to conclude that $\langle B_z \rangle$ is probably nearly constant with time. Field detection in WD 2359–434 appears reasonably secure, and the two measurements obtained so far are consistent with a field nearly constant with time. The hotter stars WD 0446–789, WD 1105–048, and 40 Eri B, appear to have variable fields.

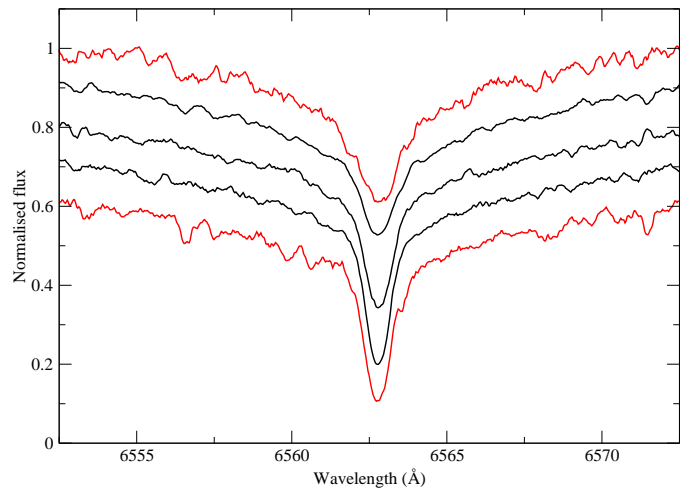


Fig. 3. $H\alpha$ cores of four hot white dwarfs. Top to bottom: WD 0446–789 (magnetic according to Table 2, red line), WD 1620–391, WD 2039–202, WD 2007–303 (all with longitudinal field consistent with zero), WD 1105–048 (possibly magnetic, red line).

4.4. Stokes I profiles from UVES archive data

Within the context of the SPY (Supernova Ia Progenitor survey) project (Koester et al. 2009), high-resolution UVES spectra were obtained at two different epochs for each of the stars of Table 2, except for WD 0413–077 = 40 Eri B. We downloaded all these data from the UVES archive, to look for evidence of Zeeman splitting in the $H\alpha$ line cores. The S/N in the continuum around $H\alpha$ ranges from 10 to over 100 per pixel ($= 0.03$ Å). All spectra were smoothed with a running average over nine pixels, i.e., the profiles were smoothed to an effective resolution element of about 0.27 Å, which is still small compared to the FWHM of ≈ 1 Å for even the sharpest line cores.

Figure 2 shows the $H\alpha$ line cores and inner wings of the cooler stars of Table 2, i.e., WD 2359–434, and WD 2105–820 (first and second spectra from the top, respectively, in red). Both of these spectra show evidence of Zeeman splitting. For comparison, Fig. 2 also shows the spectra of two non-magnetic cool white dwarfs of Table 1, WD 1826–045 and WD 1952–206 (third and fourth lines from top, respectively). The $H\alpha$ cores of the two latter WDs show no significant excess width beyond that due to pressure broadening (see discussion by Koester et al. 1998).

As discussed in Sect. 3.1, Zeeman splitting of the $H\alpha$ core of WD 2105–820 was already suspected by Koester et al. (1998); in the UVES data, with the smoothing adopted in Fig. 2, the line core appears fairly clearly split into the π and two σ components due to the Zeeman effect. The magnetic field of this star is further discussed in Sect. 5.

WD 2359–434 has been discussed by Koester et al. (1998) and by Koester et al. (2009), who interpret the profile as showing a sharp central π component and two broad σ components, which suggests a rather non-uniform field with a mean value of $\langle |B| \rangle \approx 100$ kG. A comparison between the two available UVES spectra (which were obtained four days apart) shows evidence of slight variability. The small value of the ratio $\langle B_z \rangle / \langle |B| \rangle \sim 0.04$ suggests either that, if the field is roughly dipolar, we are looking at it from nearly in the plane of the magnetic equator, or that the field may be substantially more com-

plex than a dipolar field, perhaps somewhat like WD 1953–011 (Valyavin et al. 2008).

Figure 3 shows the $H\alpha$ cores for five hotter stars of Table 2. The top spectrum is that of WD 0446–789, which according to Table 2 has a field with $\langle B_z \rangle$ up to -6 kG. The $H\alpha$ line core appears to show significant excess broadening compared to the others, probably due to Zeeman splitting corresponding to a 20 to 30 kG field. The two available UVES spectra, separated by a time interval of about four days, show only marginal signs of variability. The relatively high ratio $|\langle B_z \rangle|/\langle |B| \rangle$ suggests that the star might have a roughly dipolar morphology, with a polar field strength of order 30 to 40 kG.

The remaining four $H\alpha$ line cores of Figure 3 show no evidence of Zeeman splitting, and none of them show any variation with time. Three of these spectra are those of stars which have longitudinal magnetic field consistent with zero (WD 1620–391, WD 2039–202, and WD 2007–303). The fourth unresolved core (the lowest in the Figure) is that of WD 1105–048, which according to Table 2 has a field for which $\langle B_z \rangle$ ranges between -8 and $+3$ kG. With $\langle B_z \rangle$ this large, we would expect a $\langle |B| \rangle$ value of the order of at least about 20 kG, or even more. It is therefore rather surprising that UVES spectra do not show any sign of Zeeman broadening or splitting.

5. A simple magnetic model for WD 2105–820

WD 2105–820 is the only kG MWD for which there exists a sufficiently large number of magnetic field measurements to allow us to start simple modelling.

Four of our longitudinal field measurements were obtained during one week, and the fifth one about one month later. During this time interval, the field shows at most marginal evidence of variability, and the observed fluxes show none.

Mean field modulus measurements made by Koester et al. (1998) from CASPEC observations of excess $H\alpha$ line core broadening (which we can now safely ascribe to the Zeeman effect) yield a field strength $\langle |B| \rangle$ of 43 ± 10 kG. Although all three observations have very low S/N, it appears that the three $H\alpha$ profiles show similar Zeeman broadening. The first two measurements were obtained on 1995 July 13, and the last on 1996 July 29, i.e., about a year later (D. Koester, private communication). In addition, two further high-resolution spectra of this star containing $H\alpha$ were obtained with UVES for the SPY project (Koester et al. 2009), one on 2002 May 29, and one on 2003 May 13 (see Sect. 4.4). Koester et al. (2009) remark that the excess broadening of $H\alpha$ in these spectra is very similar in width to that observed in the three older spectra, and thus they find no evidence that $\langle |B| \rangle$ has changed. The S/N of the 2003 spectrum is too low to make possible an accurate determination of $\langle |B| \rangle$, but in the 2002 spectrum, the $H\alpha$ core appears to show the π and two σ components clearly, with a $\sigma - \sigma$ separation of ~ 1.7 Å, corresponding to $\langle |B| \rangle = 42 \pm 3$ kG. Since the available Stokes I measurements were obtained over a span of eight years, we conclude that the observed mean field modulus of WD 2105–820 does not change much even over a time scale of a decade.

Assuming that the star’s magnetic model can be described in terms of the oblique rotator model, which seems to be generally true of MWDs that have been modelled in detail (Landstreet 1992; Külebi et al. 2009b), these results indicate that either (1) the stellar rotation period is much longer than one year (or possibly shorter than the integration time of the observations), or that the magnetic structure is such that the observed field does not vary much as the star rotates, i.e., (2) the field is roughly sym-

metric about the rotation axis, or (3) the rotation axis is nearly aligned to the line of sight.

We note that none of the variable MWDs with known periods discussed by Schmidt & Norsworthy (1991) or Kawka et al. (2007) (see also Table 2 of Landstreet 1992) have rotation periods longer than 18 days (and only one has a rotation period significantly shorter than 1 hr). Thus we consider the hypothesis of a field approximately symmetric about the star’s rotation axis, or possibly of a stellar rotation axis nearly parallel to the line of sight.

We furthermore note that the value of the ratio $\langle B_z \rangle/\langle |B| \rangle \approx 0.22$ is a strong indicator of a rather simple magnetic field structure (a much smaller value is expected for complex fields such as those of solar-type stars). In particular, the value of this ratio is consistent with a dipolar morphology (Landstreet 1988; Schmidt & Norsworthy 1991), which we adopt as a magnetic model for WD 2105–820. We note that in their modelling of DAH stars with stronger fields, Külebi et al. (2009b) frequently obtained better fits to their (time-averaged) I spectra with de-centred dipoles than with centred ones, but for the weak field of WD 2105–820 we do not have a strong constraint on possible decentring in the available data.

If we assume that the magnetic field is symmetric about the star’s rotation axis, then the dipolar axis must be parallel to the stellar rotation axis. Using Eqs. (1), (2), (6), (8), and (21) of Hensberge et al. (1977) (setting the limb darkening coefficient to 1, $\langle B_z \rangle = \text{const} = 10$ kG, $\langle |B| \rangle = \text{const} = 43$ kG), we find that the observations are consistent with a simple centred dipole with a polar field strength of ~ 56 kG, and magnetic axis parallel to the rotation axis inclined at about $\sim 68^\circ$ with respect to the line of sight. If we assume a rotation axis parallel to the line of sight, then magnetic field observations are explained again by a dipole with field strength at the pole of ~ 56 kG, but with dipole axis tilted at $\sim 68^\circ$ with respect to the rotation axis (which is parallel to the line of sight). Note that the field models obtained in the two cases are the same; the only difference between the models is that the inclination of the rotation axis to the line of sight i , and the obliquity angle between the rotation and dipole axes β , have been exchanged.

6. Discussion and conclusions

The database that we have considered includes 20 hot DA stars (generally spectral type DA1 to DA4, $T_{\text{eff}} \gtrsim 14000$ K) and 15 cool DA stars (spectral type DA5 to DA8; $T_{\text{eff}} \lesssim 14000$ K). (We omit 40 Eri B from our sample, as we have no data to confirm the field detected, and the star was not observed in a survey of known size.) Since there are two firmly detected MWDs in each of the hot and cool samples, we conclude that detection rates are about 10% for the hot sample, and 13% for the cool sample. The small size of the sample and the small number of detections set a serious limit to accuracy of these frequency estimates. Using the Wilson 95% confidence limits (Wilson 1927), the field detection rate in hot WDs could be anywhere between 2.8 and 30%, while the field detection rate in cool DA WDs lies between 3.7 and 38%. In conclusion, the data currently available are consistent with the hypothesis that weak magnetic fields occur with the same frequency in hot and cool DA WDs. Globally, the detection of four weak magnetic fields from a total sample of 36 WDs makes it quite clear that the probability of finding a weak field in a DA WD is neither negligible, nor close to 1; at the 95% confidence limits, the probability lies between 4 and 25%. Therefore, it appears that the probability of detecting a ~ 10 kG field in a WD is comparable to the probability of detect-

ing a magnetic field with strength in the range 100 kG – 500 MG, which is $\sim 10\%$.

Re-addressing some of the questions posed in Sect. 1, it appears now that ~ 10 kG longitudinal fields are not ubiquitous in WDs lacking stronger fields, nor do fields seem to die away at this level. Furthermore, we have not found any significant difference between field detection rates in cool, old WDs and field detection rate in hot, young WDs. Studying these questions further will require substantially larger samples of precise field measurements than those available now.

The results of this paper highlight the need for (1) further field measurement of the MWDs already detected in this low-field regime, to fully confirm the reported detections, and to provide data on possible variability in order to characterise the field structures observed; (2) an extended high-precision survey of magnetic fields in hot and cool WDs, aimed at refining the frequency of occurrence of weak fields in the range studied here; and (3) a still deeper survey, using long integrations, to reach even weaker fields (note that standard errors of 300 – 500 G are already achieved in a number of stars with integrations of mostly less than 30 min). It will also be interesting to discover whether the morphologies of the fields of kG MWDs are often roughly symmetric about the rotation axis, as seems to be the case for WD 2105–820 and as frequently happens for MWDs with stronger fields. All of these goals are within reach of observing programmes on the VLT with FORS2, although they would be very difficult on smaller telescopes.

After this paper was accepted, S. Vennes communicated to us the results of a survey of magnetic fields in a sample of 58 proper motion white dwarfs (Kawka & Vennes 2012). The stars of their survey are complementary to the two samples discussed in our paper. Our hot sample contains stars with typical cooling ages of 300 Myr or less, and our cool sample WDs typically have cooling ages of 300 – 1000 Myr, while the sample of Kawka & Vennes is made up largely of stars with cooling ages above 1 Gyr. Because the WDs observed by Kawka & Vennes are both cooler and typically 2–3 mag fainter than those of our samples, their median standard error of field measurement is about 3 kG, compared to about 800 G for our sample. They are thus sensitive mainly to $\langle B_z \rangle$ fields larger than 10–20 kG, just above the $\langle B_z \rangle$ range of greatest interest to our study. However, their results seem to be significantly different from ours, as they find a probability of field detection of the order of 1 – 2% per decade of field strength, while the samples discussed by us suggest probabilities of the order of 10% per decade in the weak-field limit. Further observations will be needed to determine if this difference is real. If the difference is indeed real, it may be an evolutionary effect of field decay with time, or a real increase in probability as we probe smaller and smaller field strengths.

Acknowledgements. We thank the referee, Prof. Gary Schmidt, for a careful reading of the manuscript and for helpful comments. JDL and GAW acknowledge financial support from the Natural Sciences and Engineering Research Council of Canada.

References

- Aurière, M., Wade, G. A., Silvester, J. et al. 2007, *A&A*, 475, 1053
 Aznar Cuadrado, R., Jordan, S., Napiwotzki, R. et al. 2004, *A&A*, 423, 1081
 Bagnulo, S., Landolfi, M., Landstreet, J. D. et al. 2009, *PASP*, 121, 993
 Bagnulo, S., Landstreet, J. D., Fossati, L., Kochukhov, O. 2012, *A&A*, 538A, 129
 Fabrika, S. N., Valyavin, G. G., Burlakova, T. E. 2003, *AstL*, 29, 737
 Greenstein, J. L. 1984, *ApJL*, 281, L47
 Giammichele, N., Bergeron, P., Dufour, P. 2012, *ApJS*, 199, 29
 Jordan, S. 1992, *A&A*, 265, 570
 Jordan, S., Aznar Cuadrado, R., Napiwotzki, R., Schmid, H. M., Solanki, S. K. 2007, *A&A*, 462, 1097
 Jordan, S., Bagnulo, S., Klaus, W., & O’Toole, S.J. 2012, *A&A*, 542, 64
 Hensberge, H., van Rensbergen, W., Deridder, G., & Goossens, M. 1977, *A&A*, 61, 235
 Kawka, A., Vennes, S., Schmidt, G. D., Wickramasinghe, D. T., Koch, R. 2007, *ApJ*, 654, 499
 Kawke, A., Vennes, S. 2012, *MNRAS*, in press
 Kemp, J. C., Swedlund, J. B., Landstreet, J. D., Angel, J. R. P. 1970, *ApJ*, 161, L77
 Koester, D., Dreizler, S., Weidemann, V., Allard, N. F. 1998, *A&A*, 612
 Koester, D., Voss, B., Napiwotzki, R. et al. 2009, *A&A*, 505, 441
 Külebi, B., Jordan, S., Euchner, F., Hirsch, H., Löffler, W. 2009, *JPhCS*, 172a, 2047
 Külebi, B., Jordan, S., Euchner, F., Gänsicke, B. T., Hirsch, H. 2009, *A&A*, 506, 1341
 Lajoie, C.-P., Bergeron, P. 2007, *ApJ*, 667, 1126
 Landstreet, J. D. 1982, *ApJ*, 258, 639
 Landstreet, J. D. 1988, *ApJ*, 326, 967
 Landstreet, J. D. 1992, *A&AR*, 4, 35
 Landstreet, J. D., Bagnulo, S., Fossati, L., Jordan, S., & and O’Toole, S.J. 2012, *A&A*, 541, A100
 Liebert, J. 1988, *PASP*, 100, 1302
 Liebert, J., Bergeron, P., Holberg, J. B. 2003, *ApJ*, 125, 248
 Schmidt, G. D. 2001, *ASPCs*, 248, 443
 Schmidt, G. D., Norsworthy, Jane E. 1991, *ApJ*, 366, 270
 Valyavin, G. G., Fabrika, S. N. 1998, *BSAO*, 45, 69
 Valyavin, G., Bagnulo, S., Fabrika, S. et al. 2006, *ApJ*, 648, 559
 Valyavin, G., Wade, G. A., Bagnulo, S. et al. 2008, *ApJ*, 683, 466
 Wickramasinghe, D. T. & Ferrario, L. 1988, *ApJ*, 327, 222
 Wilson, E. B. 1927, *J. Am. Stat. Assn.* 22, 209

Table 3. Revised $\langle B_z \rangle$ field strength values for all magnetic field measurements of potential kG field DA white dwarfs, obtained from H Balmer lines only

Star names	Spec. type	T_{eff} (K)	$\log g$	ESO Pr. ID	MJD	t_{int} (s)	$\langle B_z \rangle$ (G)	field detected?	
WD 0135-052	NLTT 5460	DA7	7273	7.85	070.D-0259	52608.097	1828	-555 ± 530	N
WD 0227+050	GJ 100.1	DA3	18887	7.84	070.D-0259	52637.120	2292	671 ± 590	N
						52669.062	2292	-524 ± 580	
WD 0310-688	GJ 127.1	DA3	15658	8.09	070.D-0259	52695.054	1680	85 ± 420	N
WD 0346-011	GD 50	DA1	41196	9.15	070.D-0259	52637.176	2800	1307 ± 3540	N
						52674.078	2800	-1818 ± 3780	
WD 0446-789	BPM 3523	DA3	23627	7.69	070.D-0259	52609.229	2800	-2548 ± 820	Y
						52668.087	2800	-5670 ± 935	
WD 0612+177	NLTT 16280	DA2	25312	7.94	070.D-0259	52609.274	2800	-1445 ± 725	N
						52672.079	2800	-341 ± 730	
WD 0631+107	KPD 0631+1043	DA2	26718	7.87	070.D-0259	52700.130	2800	-1182 ± 1100	N
						52702.125	2800	335 ± 1095	
WD 0839-327	LTT 3218	DA6	9318	7.99	070.D-0259	52608.319	1870	315 ± 250	N
WD 0859-039	WD J0902-041	DA2	23731	7.79	070.D-0259	52674.227	2320	-148 ± 770	N
						52696.219	2320	-1168 ± 735	
WD 1042-690	NLTT 25239	DA3	21012	7.93	070.D-0259	52668.351	2562	-1008 ± 755	N
						52674.273	2562	503 ± 755	
						52695.301	2562	27 ± 575	
WD 1105-048	NLTT 26379	DA3	15142	7.85	070.D-0259	52641.351	1948	59 ± 580	P
						52669.305	1948	3341 ± 655	
WD 1202-232	EC12028-2316	DA	8615	8.04	073.D-0356	53144.146	2000	-392 ± 605	N
						53147.179	2000	-383 ± 435	
						53150.997	2000	-343 ± 440	
WD 1327-083	G 14-58	DA4	13823	7.80	073.D-0356	53151.033	1740	-201 ± 480	N
						53153.068	1710	149 ± 485	
WD 1334-678	LTT 5267	DA6	8769	7.93	073.D-0516	53134.050	1384	4017 ± 3285	N
						53137.010	1384	-5021 ± 4210	
WD 1425-811	LTT 5712	DA6	12098	8.21	073.D-0516	53137.044	960	488 ± 1360	N
WD 1620-391	CD-38 10980	DA2	24231	8.07	069.D-0210	52383.426	240	223 ± 775	N
						52383.431	300	703 ± 1110	
					073.D-0356	53136.301	1022	188 ± 335	
						53143.322	1022	184 ± 500	
						53147.255	1022	-12 ± 315	
						53151.070	1022	-48 ± 420	
WD 1733-544	LTT 6999	DA8	6165	7.23	073.D-0516	53199.178	1664	4104 ± 4390	N
WD 1826-045	LTT 7347	DA6	9057	7.91	073.D-0516	53193.179	1920	-2705 ± 1535	N
WD 1845+019	LAN 18	DA2	29384	7.81	073.D-0356	53131.395	2100	76 ± 855	N
						53136.389	2100	99 ± 755	
WD 1919+145	GD 219	DA5	14430	8.06	073.D-0356	53132.324	2100	-1451 ± 790	N
						53136.351	2100	-953 ± 760	
WD 1952-206	LTT 7873	DA6	13184	7.82	073.D-0516	53251.088	2840	530 ± 1180	N
WD 2007-303	LTT 7987	DA4	14454	7.86	067.D-0306	52076.437	200	2058 ± 2670	N
					073.D-0356	53132.382	3600	501 ± 360	
						53138.373	1800	-490 ± 400	
WD 2014-575	RE J2018-572	DA2	27465	7.94	073.D-0356	53140.360	2100	730 ± 1075	N
						53184.273	700	-5213 ± 2235	
						53185.107	2100	-697 ± 1230	
WD 2039-202	LTT8189	DA3	19188	7.93	060.A-9203	53869.443	851	-4367 ± 1915	N
					073.D-0322	53148.420	532	944 ± 770	
					073.D-0356	53143.362	1800	-288 ± 645	
						53167.393	1800	604 ± 400	
WD 2105-820	LTT 8381	DA6	10794	8.19	073.D-0516	53192.269	1760	9274 ± 1375	Y
						53193.278	1760	11423 ± 995	
						53197.294	880	8173 ± 1630	
						53199.317	880	9130 ± 1490	
						53227.209	1760	9770 ± 845	
WD 2115-560	LTT 8452	DA6	9625	8.01	073.D-0516	53199.342	1664	-1367 ± 1065	N
						53227.238	1664	132 ± 955	
WD 2149+021	G 93-48	DA3	17360	7.93	073.D-0356	53183.278	2088	-875 ± 675	N

Table 3. Table 3., continued

Star names		Spec. type	T_{eff} (K)	$\log g$	ESO Pr. ID.	MJD	t_{int} (s)	$\langle B_z \rangle$ (G)	field detected?
						53196.346	2088	354 ± 575	
						53222.200	2088	2 ± 540	
WD 2151-015	NLTT 52306	DA6	9194	7.97	073.D-0516	53240.174	1840	3941 ± 1910	N
						53251.124	1840	-2027 ± 950	
						53252.120	1840	-688 ± 1660	
WD 2211-495	RE J2214-491	DA	62236	7.54	073.D-0356	53140.401	1610	819 ± 1095	N
						53185.246	1610	-576 ± 1205	
WD 2333-049	G 157-82	DA6	10608	8.04	073.D-0516	53274.201	1704	5102 ± 5550	N
WD 2359-434	LTT 9857	DA5	8544	8.44	070.D-0259	52583.025	2188	4097 ± 840	Y
						52608.056	2188	3090 ± 510	

List of Objects

- 'WD 2105-820' on page 1
- 'WD 2359-434' on page 1
- 'WD 2151-015' on page 3
- 'WD 0446-789' on page 4
- 'WD 1105-048' on page 4
- 'WD 1620-391' on page 4
- 'WD 2007-303' on page 4
- 'WD 2039-202' on page 4
- 'WD 0413-077' on page 4
- 'WD 1826-045' on page 5
- 'WD 1952-206' on page 5
- 'WD 1953-011' on page 6
- 'WD 1620-391' on page 6
- 'WD 2007-303' on page 6